

GAIA-DR2 CONFIRMS VLBA PARALLAXES IN OPHIUCHUS, SERPENS AND AQUILA

GISELA N. ORTIZ-LEÓN¹, LAURENT LOINARD^{2,3}, SERGIO A. DZIB¹, MARINA KOUNKEL⁴, PHILLIP A. B. GALLI⁵, JOHN J. TOBIN^{6,7}, NEAL J. EVANS II⁸, LEE HARTMANN⁹, LUIS F. RODRÍGUEZ², CESAR BRICEÑO¹⁰, ROSA M. TORRES¹¹ AND AMY J. MIODUSZEWSKI¹²

¹Max Planck Institut für Radioastronomie, Auf dem Hügel 69, D-53121 Bonn, Germany

²Instituto de Radioastronomía y Astrofísica, Universidad Nacional Autónoma de México, Morelia 58089, Mexico

³Instituto de Astronomía, Universidad Nacional Autónoma de México, Apartado Postal 70-264, 04510 Ciudad de México, México

⁴Department of Physics and Astronomy, Western Washington University, 516 High St, Bellingham, WA 98225, USA

⁵Laboratoire d'astrophysique de Bordeaux, Univ. Bordeaux, CNRS, B18N, allée Geoffroy Saint-Hillaire, 33615 Pessac, France.

⁶Homer L. Dodge Department of Physics and Astronomy, University of Oklahoma, 440 W. Brooks Street, Norman, OK 73019, USA

⁷Leiden Observatory, PO Box 9513, NL-2300 RA, Leiden, The Netherlands

⁸Department of Astronomy, The University of Texas at Austin, 2515 Speedway, Stop C1400, Austin, TX 78712-1205, USA

⁹Department of Astronomy, University of Michigan, 500 Church Street, Ann Arbor, MI 48105, USA

¹⁰Cerro Tololo Interamerican Observatory, Casilla 603, La Serena, Chile

¹¹Centro Universitario de Tonalá, Universidad de Guadalajara, Avenida Nuevo Periférico No. 555, Ejido San José Tatepozco, C.P. 48525, Tonalá, Jalisco, México.

¹²National Radio Astronomy Observatory, Domenici Science Operations Center, 1003 Lopezville Road, Socorro, NM 87801, USA

ABSTRACT

We present Gaia-DR2 astrometry of a sample of YSO candidates in Ophiuchus, Serpens Main and Serpens South/W40 in the Aquila Rift, which had been mainly identified by their infrared excess with *Spitzer*. We compare the Gaia-DR2 parallaxes against published and new parallaxes obtained from our Very Long Baseline Array (VLBA) program GOBELINS. We obtain consistent results between Gaia and the VLBA for the mean parallaxes in each of the regions analyzed here. We see small offsets, when comparing mean values, of a few tens of micro-arcseconds in the parallaxes, which are either introduced by the Gaia zero-point error or due to a selection effect by Gaia toward the brightest, less obscured stars. Gaia-DR2 data alone conclusively places Serpens Main and Serpens South at the same distance, as we first inferred from VLBA data alone in a previous publication. Thus, Serpens Main, Serpens South and W40 are all part of the same complex of molecular clouds, located at a mean distance of 436 ± 9 pc. In Ophiuchus, both Gaia and VLBA suggest a small parallax gradient across the cloud, and the distance changes from 144.2 ± 1.3 pc to 138.4 ± 2.6 pc when going from L1689 to L1688.

Keywords: astrometry - radiation mechanisms: non-thermal - radio continuum: stars - techniques: interferometric - ISM: individual objects: Aquila Rift complex - ISM: individual objects: Ophiuchus

1. INTRODUCTION

Observations of nearby regions rich in extremely young objects (for example Ophiuchus, Perseus, Taurus, Orion, Serpens, etc.) provide a wealth of information and clues to understand the paradigm for star formation. In this context, the knowledge of the distance to star-forming regions is essential for properly interpreting the observed properties of young objects, from pre-stellar

cores to disks, as well as their environment. An advance in constraining the distance of these star-forming regions has been made with astrometric observations using Very Long Baseline Interferometry (VLBI; see for example Reid & Honma 2014). In particular, our team has conducted a major program to measure individual distances during the last few years, via the trigonometric parallax, and proper motions to almost a hundred young stars in such nearby star-forming regions (the Gould's Belt Distances Survey – GOBELINS; Loinard 2013). The distance to young stars in Ophiuchus (Ortiz-León et al. 2017a), Serpens (Ortiz-León et al. 2017b),

Orion (Kounkel et al. 2017), Taurus (Galli et al. 2018) and Perseus (Ortiz-León et al. 2018) is now known with 0.2 – 3% accuracy, yielding relevant information about their three-dimensional structure.

On 2018, April 25 the Gaia mission published its second Data Release (DR2; Lindegren et al. 2018; Gaia Collaboration et al. 2018). This release contains astrometric solutions for more than 1.3 billion stars with parallax uncertainties of ~ 0.7 mas for a magnitude $G = 20$. Several young stars within the star-forming regions studied by our program have parallax and proper motions measurements available in the DR2 catalog. Therefore, we can now compare the VLBI astrometry against Gaia, to validate the accuracy of our measurements.

Here we analyze Gaia-DR2 and VLBA astrometry in Ophiuchus, Serpens and the Aquila Rift. Ophiuchus consists of a main cloud known as Lynds 1688 (L1688; see e.g. Wilking et al. 2008 for a recent review) and several filamentary clouds to the northeast (L1709 and L1704) and the southeast (L1689, L1712 and L1729). The Serpens Molecular cloud and the Aquila Rift are two cloud complexes projected close to each other in the plane of the sky. The well studied Serpens Main cluster is embedded within the Serpens Molecular cloud (Eiroa et al. 2008), while W40 (Smith et al. 1985) and the extremely young Serpens South cluster (Gutermuth et al. 2008) are embedded within the Aquila Rift, about 3° to the south of Serpens Main. Because Serpens South has the most star-formation activity within the Aquila, it is often referred to as the Aquila or the Serpens-Aquila region (e.g. within the *Herschel* Gould Belt Survey program; André et al. 2010).

2. VLBA OBSERVATIONS

New Very Long Baseline Array (VLBA) observations toward Ophiuchus, Serpens Main and W40 (within the Aquila Rift) were performed in the period from 2016, August to 2018, October under project code BL175. These data were taken at 5 GHz following the observing strategy described in detail in Ortiz-León et al. (2017a) and Ortiz-León et al. (2017b, hereafter Papers I and II, respectively).

The resulting astrometric parameters from the updated fits, including new sources, are given in Table 1. In addition to the 24 objects published in Papers I and II, here we present new parallaxes for 6 objects. Following the approach outlined in Loinard et al. (2007), the data are fitted with a model that assumes a uniform proper motion and has the following free parameters: parallax (ϖ), proper motions (μ_α, μ_δ) and position at the reference epoch (α_0, δ_0). The fits to sources that are members of wide binary systems also include acceleration terms, (a_α, a_δ). We also update the orbital fits of our binary systems following Kounkel et al. (2017),

however, in this paper we will focus solely on parallax, and leave the discussion on the orbital parameters for a forthcoming publication.

For Ophiuchus, the weighted mean of individual parallaxes in each cloud gives $\varpi = 7.23 \pm 0.14$ mas and $\varpi = 6.93 \pm 0.06$ mas, for L1688 and L1689, respectively. Herein, and in the rest of the paper, the quoted errors on weighted mean parallaxes correspond to the standard deviation, unless otherwise noted. These measurements suggest that, although small, there is a parallax gradient across this cloud, but the difference in parallax is only significant at 2σ .

In Serpens/Aquila, we found $\varpi = 2.31 \pm 0.01$ mas and $\varpi = 2.23 \pm 0.10$ mas, for the Serpens Main and W40 clusters, respectively. In this case, the mean parallaxes are consistent between them within 1σ . The average of all sources in both regions gives $\varpi = 2.30 \pm 0.05$ mas.

3. ANALYSIS OF GAIA DR2 DATA

We use the list of young stellar object (YSO) candidates derived with *Spitzer* by Dunham et al. (2015) for Ophiuchus (292 sources), Serpens (227 sources) and Aquila (1319 sources). However, this sample suffers from contamination by background AGB stars (between 25% and 90%; Dunham et al. 2015), so their membership and nature as true YSOs must be confirmed. We also use the list of 316 YSOs compiled by Wilking et al. (2008) for Ophiuchus, which are all 2MASS sources within the L1688 cloud, with detection in the K_S band and other signs of youth, such as H_α or X-ray emission. The combined sample has 565 YSO candidates in Ophiuchus.

We cross-matched the positions of the YSO candidates against Gaia DR2 positions using a search radius of $1''$ and the Virtual Observatory tool TOPCAT (Taylor 2005). In Ophiuchus, 191 sources of the *Spitzer*+2MASS catalog have astrometric solutions. The distribution of Gaia parallaxes is shown in Figure 1 (left panel) and their positions on the plane of the sky in Figure 2. We note that this sample contains background and foreground contaminants with parallaxes ≤ 3 and ≥ 11 mas (i.e. well outside the range from 120 to 150 pc reported in the literature as the distance to Ophiuchus). To remove these stars, we look at the distributions of proper motions and, following Ortiz-León et al. (2018) and Dzib et al. (2018), we cut all stars with proper motions outside 3σ from the mean, as determined by fitting a Gaussian model to the measured proper motions in each direction. Then, we produce a sample with reliable parallaxes by applying the recommended cuts given in Lindegren et al. (2018), which are designed to remove sources with poor or spurious astrometric solutions. Specifically, we applied the criteria expressed in equations C.1 and C.2 in appendix C of Lindegren et al. (2018). After cutting also sources that lie well outside the region shown in

Figure 2 (2 sources at $(\alpha, \delta) \sim (252^\circ, -14^\circ)$) the sample is reduced to 107 objects. The resulting weighted mean parallax for this reduced sample is 7.23 ± 0.25 mas.

To compare against the VLBA parallaxes, we bin the Gaia parallaxes into R.A. bins of width equal to 0.5° , and take the weighted average of the parallaxes within each bin. The resulting values are plotted in Figure 2 as yellow triangles. The weighted parallaxes for the two first bins are 6.82 ± 0.40 and 6.88 ± 0.13 mas, respectively, which agree within the errors with the VLBA parallax derived for L1689 (6.93 ± 0.06 mas). Gaia data also suggest that the parallaxes at the center of L1688 are, on average, slightly larger than L1689. The weighted average parallax rises to 7.31 ± 0.21 mas roughly at the center of L1688.

For Aquila, we found 341 YSO candidates with available parallaxes in DR2. We can see in the middle panel of Figure 1 that the number of background contaminants is remarkably high for this region ($\sim 80\%$ of the total), and the presence of two distributions, with peaks separated at $\varpi \sim 2$ mas, is clear. The stars with small parallaxes almost follow a Gaussian distribution as can be seen in the same figure. The center of this Gaussian is at $\varpi = 0.09 \pm 0.03$ mas and the width is 0.46 mas. From this figure we can assume that all stars with $\varpi \lesssim 1.4$ mas, which is the boundary between the Gaussian and the second distribution, are background contaminants. We then cut further the sample by applying the proper motion criterium and the criteria to filter stars with spurious astrometric solutions as in Ophiuchus. This produced the reduced sample of 24 stars shown in Figure 3, where we see that stars are grouped in at least three regions. One group of stars is distributed within a diameter of ~ 2 degrees around the position $(\alpha, \delta) \sim (277.6^\circ, -2.3^\circ)$, encompassing the W40 and Serpens South clusters. A second group of stars is located around the position $(\alpha, \delta) \sim (279^\circ, +0^\circ)$. The next group is centred at $(\alpha, \delta) \sim (277^\circ, -4^\circ)$ and finally one more star is close to $(\alpha, \delta) \sim (271^\circ, -4.5^\circ)$.

Similarly to Ophiuchus, we bin the Gaia parallaxes into R.A. and declination bins of width equal to 1° and 2° , respectively. We then take the weighted average in each bin (the yellow triangles in Figure 3). The groups identified above in the spatial distribution of the Gaia parallaxes are clearly seen in the plot corresponding to the declination direction (right panel in Figure 3). The weighted mean of stars within a radius of 1 degree around $(\alpha, \delta) \sim (277.6^\circ, -2.3^\circ)$, i.e. the area covering the W40 and Serpens South clusters and corresponding to the second yellow triangle in the right panel of Figure 3, gives $\varpi = 2.31 \pm 0.22$ mas. This is the representative Gaia value that we take for W40/Serpens South.

In Serpens, only 68 *Spitzer* sources have parallaxes available in DR2. We also cross-matched the catalog

of optical candidate young stars published by [Erickson et al. \(2015\)](#), which contains 62 candidate members based on the presence of H α emission, lithium absorption, X-ray emission, mid-infrared excess, and/or reflection nebulosity. For this catalog, we use a match radius of $2''$ to be more conservative. This adds 47 stars to the number of sources with Gaia parallaxes in Serpens. The parallax distribution is shown in the right panel of Figure 1. Again, we see a peak in the parallax distribution due to background contaminants, which we remove by using the proper motion criterium. The weighted mean parallax for Serpens (of the 59 stars left after cleaning the sample from spurious astrometric solutions) gives $\varpi = 2.32 \pm 0.18$ mas. We take this value as the representative Gaia parallax for Serpens Main.

4. DISCUSSION

The Gaia-DR2 measurements confirm the results reported in Papers I and II, which were based on VLBA data alone. In paper II, we derived parallaxes for stars in W40 and Serpens Main. The VLBA parallaxes for both regions were consistent between them and suggested a common distance of ~ 436 pc. We argued that, given that Serpens South is projected very close to the W40 cluster, it should be located at the same distance of ~ 436 pc as W40, which implied that the three regions, i.e. Serpens Main, Serpens South and W40, are part of the same large complex of molecular clouds. This conclusion was supported by the similar local standard of rest (LSR) velocities obtained from observations of isotopologues of CO toward IRAS 18275–0203 and a nearby embedded source in Serpens South ([Gutermuth et al. 2008](#)) and toward various positions within the Serpens Molecular cloud ([White et al. 1995](#)).

The values of the mean parallax derived from the Gaia-DR2 data alone for Serpens South/W40 and Serpens Main ($\varpi = 2.31 \pm 0.22$ mas and $\varpi = 2.32 \pm 0.18$ mas, respectively) are identical within the errors, which conclusively places both regions at a similar distance (432_{-37}^{+45} pc and 430_{-36}^{+30} pc, respectively), i.e. at a significantly larger distance than the old, but still used by some authors, value of 260 pc ([Straizys et al. 2003](#)). As seen in the third panel of Figure 1, there is a group of stars having smaller distances ($\varpi \gtrsim 4$ mas or $d \lesssim 250$ pc), but they represent a minority compared to the main body of young stars, which draw a clear distribution around 2.3 mas.

When compared against the VLBA parallaxes, we see an offset of $\varpi_{\text{Gaia}} - \varpi_{\text{VLBA}} = +0.09 \pm 0.07$ mas and $\varpi_{\text{Gaia}} - \varpi_{\text{VLBA}} = +0.02 \pm 0.02$ mas, for W40/Serpens South and Serpens Main respectively, where ϖ_{Gaia} and ϖ_{VLBA} are the weighted mean parallax for Gaia and the VLBA, respectively. In Ophiuchus, we measure offsets of $\varpi_{\text{Gaia}} - \varpi_{\text{VLBA}} = +0.06 \pm 0.02$ mas and

$\varpi_{\text{Gaia}} - \varpi_{\text{VLBA}} = -0.07 \pm 0.04$ mas, in L1688 and L1689, respectively. Although these offsets are relatively small, it is important to understand their origin. The offset measured for stars in L1689 is consistent with the zero-point error of Gaia DR2 parallaxes, which has a mean of -0.029 mas (Lindgren et al. 2018). The Gaia–VLBA parallax offset is positive in L1688, Serpens Main and the Aquila, which means that there the Gaia parallax is larger than the VLBA parallax, or that Gaia distances are, on average, smaller than the VLBA distances. This is actually the behavior we expect to see in regions where the optical extinction is high ($A_V \gtrsim 20$ as is seen in Serpens and Ophiuchus; Ridge et al. 2006; Bontemps et al. 2010). Since Gaia observes in the optical, it can only detect stars that are not too obscured by dust extinction, while the VLBA can see through the extinction wall. Thus, Gaia could be biased toward detecting stars preferentially on the near of the clouds, whereas the VLBA does not suffer from such a bias. This effect is not evident in L1689 or IC 348 in Perseus (Ortiz-León et al. 2018), where the optical extinction is lower ($A_V \lesssim 10$; Ridge et al. 2006 – see also Kounkel et al. 2018 for a parallax comparison of the whole YSOs sample in common to Gaia and GOBELINS).

Then, our findings suggest Gaia would be biased in regions with strong optical extinction. We were not able to investigate the magnitude of the bias as a function of extinction from ancillary data. Visual extinction maps available in the literature have been derived from different datasets and using different algorithms. For instance, the Ophiuchus map shown in Figure 2 was obtained from 2MASS near-infrared data, while the Serpens map (Figure 3) was derived from optical star counts and is only tracing the first layer of the extinction wall. From the distribution of the extinction measured in Ophiuchus, which increases from the east to the core of the cloud, we suggest that Gaia parallaxes on regions with $A_V \gtrsim 18$ may show a significant bias.

It is also important to note that the error bars on Gaia parallaxes are on average significantly larger than the errors on VLBA parallaxes, mainly in the Aquila Region, and that the individual Gaia values show a larger dispersion than the dispersion seen for VLBA sources. This is clearly seen in Figures 2 and 3. Quantitatively, this comes from taking the mean of Gaia parallax errors of the samples in each region before cleaning from possible poor astrometric solutions. The mean errors are $\sigma_{\varpi, \text{Gaia}} = 0.24, 0.18$ and 0.40 mas in Ophiuchus, Serpens and Aquila, respectively, while the mean of VLBA parallax errors is $\sigma_{\varpi, \text{VLBA}} = 0.12$ mas in the three regions.

Given that the Gaia zero-point offset applicable to a given region in the sky is still not well determined (Lindgren et al. 2018), and the corrections to be ap-

plied to the Gaia parallaxes are still poorly constrained, we do not attempt here to correct the Gaia parallaxes. We instead recommend to use the VLBA parallaxes and distances as they still represent the most accurate measurements obtained so far toward these three regions. Inverting the VLBA parallaxes yields distances of 138.4 ± 2.6 pc, 144.2 ± 1.3 pc and 436 ± 9 pc for L1688, L1689 and Serpens/Aquila, respectively.

Regarding the presence of parallax gradients across the clouds, we do see in Figures 2 and 3 that Gaia parallaxes change with position, rising toward the central part of the clouds, which is expected if extinction is biasing more toward the center. In Ophiuchus, VLBA parallaxes show clear variations with position along the R.A. direction, which supports the idea that different structures in the cloud are located at slightly different distances. In Serpens/Aquila, the significance of such parallax variations is low. However, we do not rule out a possible difference of ~ 16 pc between Serpens Main and Serpens South/Aquila.

To strengthen our conclusion on the distance to Aquila, we use all stars from the Gaia DR2 catalog covering a circular area with a radius of 3° and centered at $(\alpha, \delta) = (277.5, -1.0^\circ)$ (i.e., at the mid-point between Serpens Main and Serpens South). We only keep stars with $\varpi > 1$ mas ($d < 1$ kpc) and $\sigma_\varpi < 0.5$ mas, resulting in a total of 79550 stars. The spatial distribution of these stars is shown in Figure 4, where each point represents the average of all stars within small patches of size set to 500 arcsec, whose average distance (estimated as $1/\overline{\varpi}$) is indicated by a color code. We see in Figure 4 the effect of the obscuration by the cloud, because, on average, the areas with large extinction are the ones that have the lower distances. The distribution of distances is shown also in Figure 4. Here we see that the number of sources keeps rising with distance until it reaches ~ 430 pc, where there is a pause in the rise. This distance corresponds to the main distance to the cloud, which agrees very well with the distance derived from the VLBA parallax measurements.

The nature of the background *Spitzer* contaminants in Aquila is still unknown, but they are likely AGB stars according to Dunham et al. (2015). The proper motions of these stars are non-zero, which suggests they are Galactic sources.

5. CONCLUSIONS

We used Gaia-DR2 and VLBA data to investigate the distance to Ophiuchus, Serpens Main and W40/Serpens South in the Aquila Rift region. Our target samples for the Gaia analysis consisted of YSO candidates with infrared excess identified by *Spitzer*, which were complemented by including 2MASS and optical sources with other signs of an association to young

stars. We carefully cleaned our samples from background and foreground stars, and from stars with spurious astrometric solutions, and then derived the weighted mean parallax of each region. From Gaia data alone, we found identical parallaxes for both Serpens Main ($\varpi_{\text{Gaia}} = 2.32 \pm 0.18$ mas) and W40/Serpens South ($\varpi_{\text{Gaia}} = 2.31 \pm 0.22$ mas), which are consistent with the parallaxes measured independently by the VLBA ($\varpi_{\text{VLBA}} = 2.30 \pm 0.05$ mas). Hence, this confirms that the three regions are part of the same complex of molecular clouds. VLBA and Gaia-DR2 parallaxes are also highly consistent between them in Ophiuchus, where we found $\varpi_{\text{L1688,VLBA}} = 7.23 \pm 0.14$ mas, $\varpi_{\text{L1689,VLBA}} = 6.93 \pm 0.06$ mas, $\varpi_{\text{L1688,Gaia}} = 7.29 \pm 0.22$ mas and $\varpi_{\text{L1689,Gaia}} = 6.86 \pm 0.23$ mas. The small offsets between Gaia and the VLBA can be understood in terms of the Gaia parallax zero point error or Gaia being biased toward the brightest and less obscured stars.

G.N.O.-L. acknowledges support from the von Humboldt Stiftung. L.L. acknowledges the financial support of DGAPA, UNAM (project IN112417), and CONACyT, México.

The Long Baseline Observatory is a facility of the National Science Foundation operated under cooperative agreement by Associated Universities, Inc. The National Radio Astronomy Observatory is a facility of the National Science Foundation operated under cooperative agreement by Associated Universities, Inc.

This work has made use of data from the European Space Agency (ESA) mission *Gaia* (<https://www.cosmos.esa.int/gaia>), processed by the *Gaia* Data Processing and Analysis Consortium (DPAC, <https://www.cosmos.esa.int/web/gaia/dpac/consortium>). Funding for the DPAC has been provided by national institutions, in particular the institutions participating in the *Gaia* Multilateral Agreement.

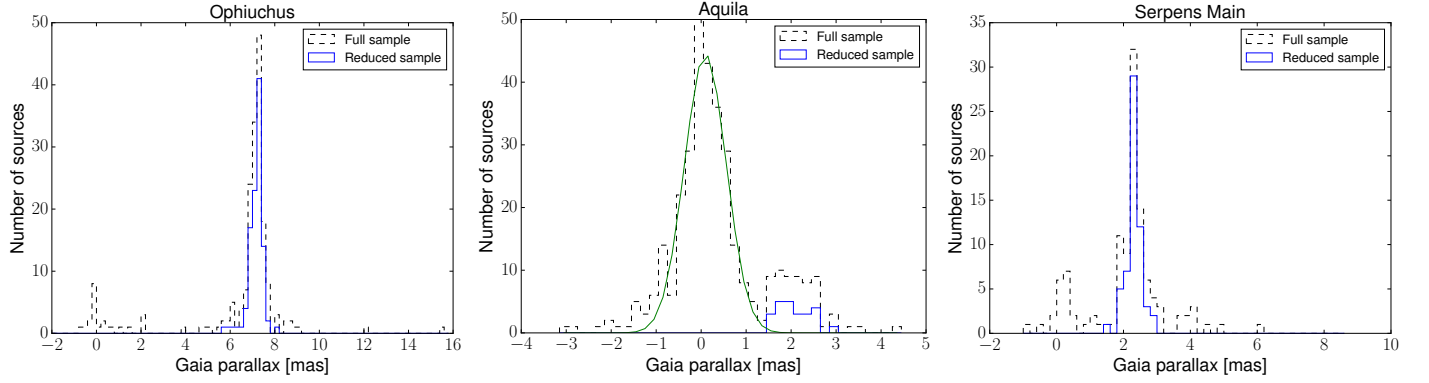


Figure 1. Gaia parallaxes from DR2 in Ophiuchus (left), Aquila (middle) and Serpens Main (right). The blue histograms show the distribution of parallaxes after cutting stars according to the criteria given in the text. The green line in the middle panel is a Gaussian fit to the parallax distribution with $\varpi \lesssim 1.4$ mas.

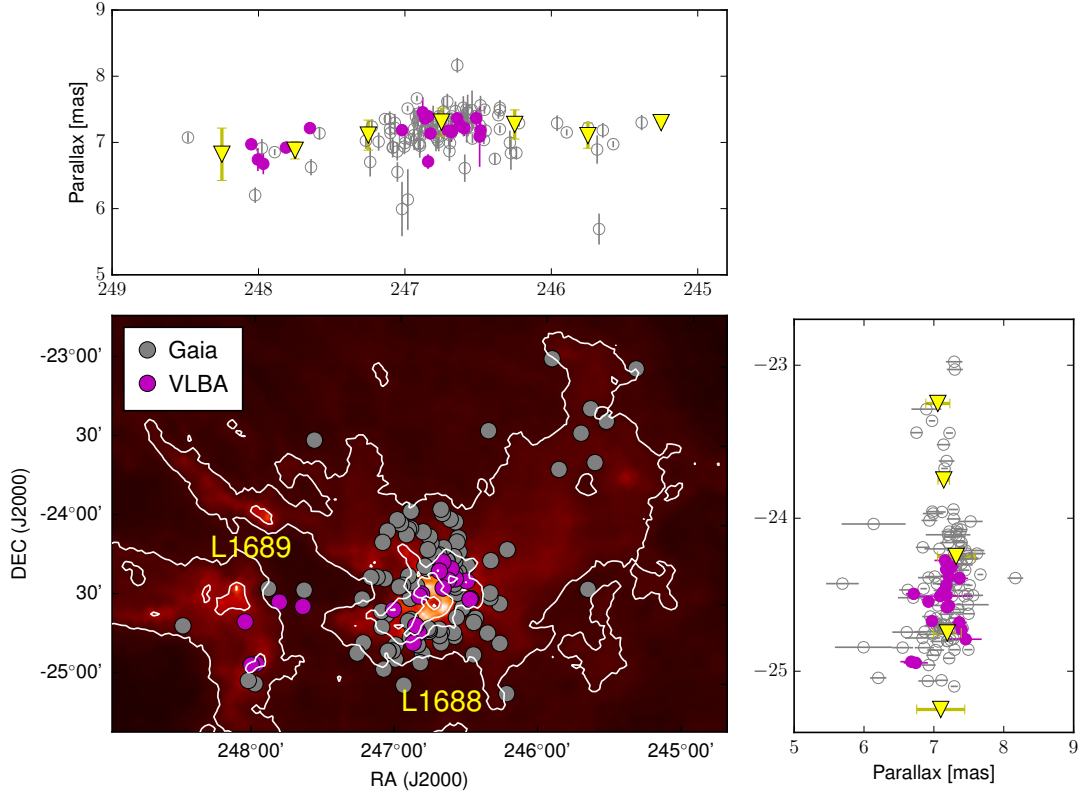


Figure 2. Gaia-DR2 and VLBA parallaxes measured in Ophiuchus. The inner panel shows the spatial distribution of stars with measured parallaxes, while the top and right panels show the parallaxes as a function of R.A. and declination, respectively. The grey open circles are stars with Gaia parallaxes, while the magenta filled circles are stars with VLBA parallaxes. The yellow triangles are the weighted mean of Gaia parallaxes determined for bins with a width of 0.5° . The map in the background is an extinction map obtained as part of the COMPLETE project (Ridge et al. 2006). The white contours indicate $A_V = 4, 12$ and 20.

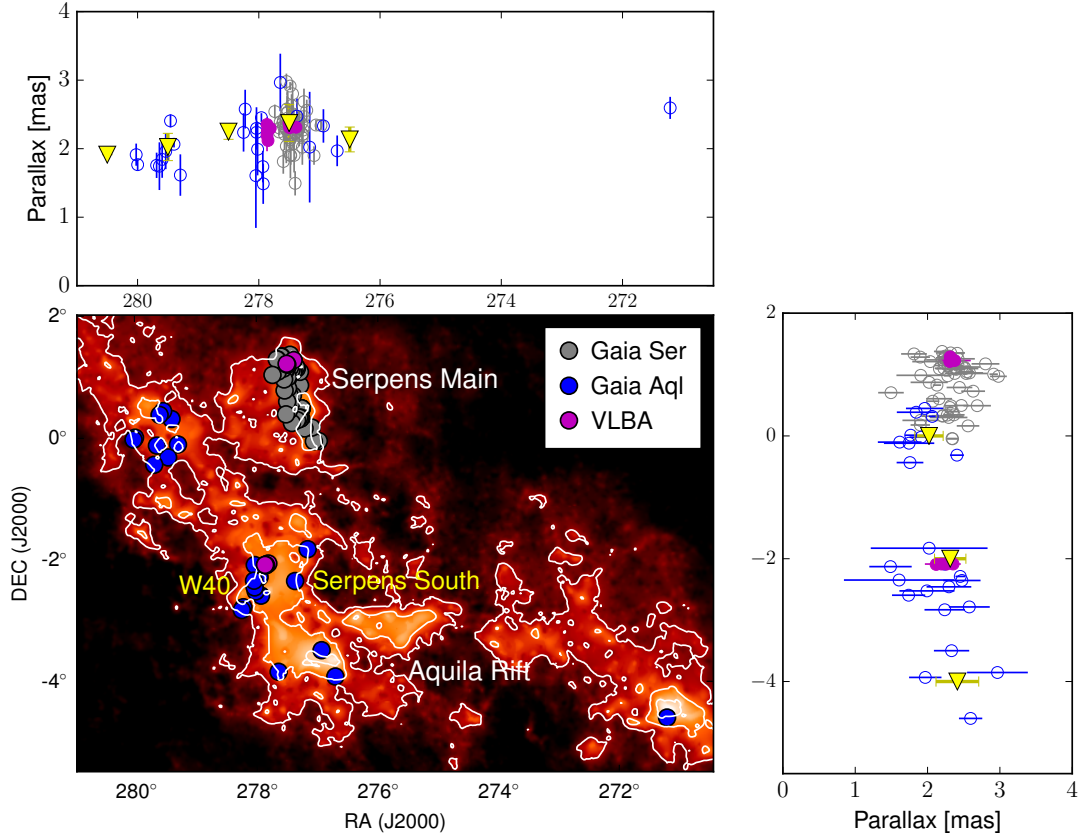


Figure 3. Same as Figure 2 but for the Serpens/Aquila region. Here the bins have widths of 1° and 2° , in R.A. and declination, respectively. The yellow triangles are the weighted mean of Gaia parallaxes in Aquila determined for these bins. Gaia parallaxes measured in Aquila are shown as blue circles. The extinction map in the background was taken from [Cambr  sy \(1999\)](#). The white contours indicate $A_V = 4, 7$ and 9 .

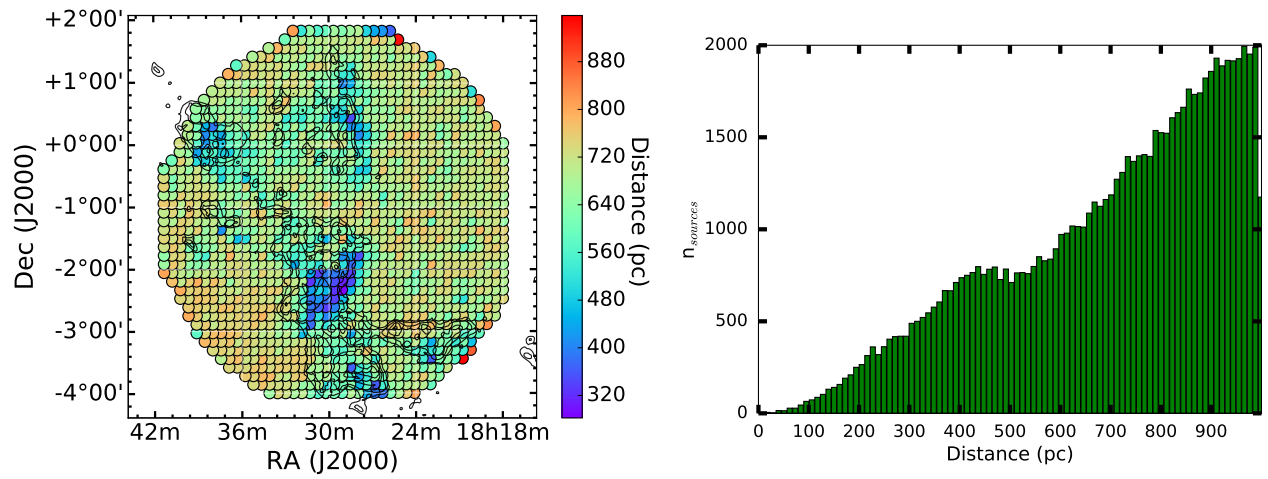


Figure 4. *Left:* Gaia-DR2 distances for all stars within 3° around $(\alpha, \delta) = (277.5, -1.0^\circ)$ and with $\varpi > 1$ mas and $\sigma_\varpi < 0.5$ mas, overlaid on the extinction map of the Aquila. Each point is the average of all stars within small patches of size set to 500 arcsec. *Right:* Histogram of distances for the same sample of stars.

Table 1. Astrometric parameters from VLBA measurements

GBS-VLA name (1)	Other identifier (2)	Parallax (mas) (3)	$\mu_\alpha \cos \delta$ (mas yr ⁻¹) (4)	μ_δ (mas yr ⁻¹) (5)	$a_\alpha \cos \delta$ (mas yr ⁻²) (6)	a_δ (mas yr ⁻²) (7)	Distance (pc) (8)
Ophiuchus							
J162556.09-243015.3	WLY2-11	7.181 ± 0.135	-8.098 ± 0.075	-21.978 ± 0.222	1.828 ± 0.14	4.264 ± 0.412	139.26 ± 2.62
J162557.51-243032.1	YLV24	7.089 ± 0.458	-7.047 ± 0.198	-25.135 ± 0.255	—	—	141.07 ± 9.12
J162603.01-242336.4	DoAr21	7.366 ± 0.123	-19.567 ± 0.064	-26.936 ± 0.056	—	—	135.76 ± 2.27
J162622.38-242253.3	LFAM2	7.216 ± 0.119	-5.622 ± 0.125	-26.658 ± 0.308	—	—	138.59 ± 2.28
J162629.67-241905.8	LFAM8	7.254 ± 0.112	-5.983 ± 0.059	-29.642 ± 0.129	—	—	137.86 ± 2.13
J162634.17-242328.4	S1	7.364 ± 0.052	-2.070 ± 0.010	-26.790 ± 0.021	—	—	135.79 ± 0.97
J162642.44-242626.1	LFAM15	7.176 ± 0.058	-6.327 ± 0.016	-26.905 ± 0.036	—	—	139.36 ± 1.13
J162643.76-241633.4	VSSG11	7.160 ± 0.152	-10.48 ± 0.16	-38.99 ± 0.35	0.31 ± 0.65	-1.54 ± 1.09	139.7 ± 3.0
J162649.23-242003.3	LFAM18	7.176 ± 0.055	-8.627 ± 0.159	-20.015 ± 1.064	—	—	139.35 ± 1.06
J162718.17-242852.9	YLV 12Bab	7.135 ± 0.064	10.875 ± 0.049	-25.057 ± 0.140	-0.622 ± 0.116	-0.177 ± 0.018	140.16 ± 1.26
J162718.17-242852.9	YLV 12Bc ¹	7.135 ± 0.064	-11.219 ± 0.052	-23.107 ± 0.128	0.195 ± 0.027	0.109 ± 0.066	140.16 ± 1.26
J162721.81-244335.9	ROXN39	7.396 ± 0.071	-6.858 ± 0.095	-24.864 ± 0.146	—	—	135.22 ± 1.30
J162721.97-242940.0	GY256	6.711 ± 0.111	-6.673 ± 0.054	-34.41 ± 0.176	—	—	149.02 ± 2.47
J162726.90-244050.8	YLV15	7.376 ± 0.095	-12.841 ± 0.042	-26.255 ± 0.169	—	—	135.57 ± 1.75
J162730.82-244727.2	DROXO71	7.455 ± 0.229	-4.822 ± 0.144	-28.256 ± 0.253	—	—	134.14 ± 4.12
J162804.65-243456.6	ROXN 78	7.185 ± 0.091	-5.446 ± 0.028	-29.301 ± 0.071	—	—	139.18 ± 1.77
J163035.63-243418.9	SFAM 87	7.216 ± 0.068	-7.702 ± 0.019	-26.028 ± 0.031	—	—	138.58 ± 1.31
J163115.01-243243.9	ROX42B	6.922 ± 0.043	-5.817 ± 0.033	-23.206 ± 0.259	-0.506 ± 0.041	0.962 ± 0.315	144.47 ± 0.91
J163151.93-245617.4	—	7.265 ± 0.778	-8.564 ± 0.268	-27.132 ± 0.589	—	—	138 ⁺¹⁷ ₋₁₃
J163152.10-245615.7	LDN1689IRS5	6.677 ± 0.157	-6.537 ± 0.09	-22.557 ± 0.144	—	—	149.76 ± 3.52
J163200.97-245643.3	WLY2-67	6.741 ± 0.173	-5.699 ± 0.14	-23.994 ± 0.357	—	—	148.34 ± 3.80
J163211.79-244021.8	DoAr51	6.972 ± 0.041	-4.746 ± 0.084	-23.139 ± 0.099	—	—	143.43 ± 0.85
Serpens Main							
J182933.07+011716.3	GFM 11	2.313 ± 0.078	3.634 ± 0.050	-8.864 ± 0.127	—	—	432 ⁺¹⁵ ₋₁₄
J182957.89+011246.0	EC 95	2.307 ± 0.022	3.579 ± 0.021	-8.359 ± 0.023	—	—	433 ± 4
J183000.65+011340.0	GFM 65	2.375 ± 0.222	2.437 ± 0.357	-8.263 ± 0.228	—	—	421 ⁺⁴⁴ ₋₃₆
W40							
J183114.82-020350.1	KGF 36	2.297 ± 0.116	0.400 ± 0.065	-6.607 ± 0.063	—	—	435 ⁺²³ ₋₂₁
J183123.62-020535.8	KGF 97	2.119 ± 0.077	-0.300 ± 0.047	-7.432 ± 0.048	—	—	472 ⁺¹⁸ ₋₁₇
J183126.02-020517.0	KGF 122	2.261 ± 0.138	1.845 ± 0.645	-6.029 ± 0.339	—	—	442 ⁺²⁹ ₋₂₅
J183127.45-020512.0	KGF 133	2.194 ± 0.231	0.181 ± 0.148	-8.750 ± 0.323	0.270 ± 0.158	-0.53 ± 0.344	456 ⁺⁵⁴ ₋₄₄
J183127.65-020509.7	KGF 138	2.353 ± 0.106	0.172 ± 0.089	-6.784 ± 0.785	—	—	425 ⁺²⁰ ₋₁₈

¹ Parallax is fixed at the value obtained for YLV 12Bab when solving for the other astrometric parameters.

REFERENCES

- André, P., Men'shchikov, A., Bontemps, S., et al. 2010, *A&A*, 518, L102
- Bontemps, S., André, P., Könyves, V., et al. 2010, *A&A*, 518, L85
- Cambrésy, L. 1999, *A&A*, 345, 965
- Dunham, M. M., Allen, L. E., Evans, II, N. J., et al. 2015, *ApJS*, 220, 11
- Dzib, S. A., Loinard, L., Ortiz-León, G. N., Rodríguez, L. F., & Galli, P. A. B. 2018, *ApJ*, 867, 151
- Eiroa, C., Djupvik, A. A., & Casali, M. M. 2008, *The Serpens Molecular Cloud*, ed. B. Reipurth, 693
- Erickson, K. L., Wilking, B. A., Meyer, M. R., et al. 2015, *AJ*, 149, 103
- Gaia Collaboration, Brown, A. G. A., Vallenari, A., et al. 2018, *A&A*, 616, A1
- Galli, P. A. B., Loinard, L., Ortiz-Lon, G. N., et al. 2018, *The Astrophysical Journal*, 859, 33
- Gutermuth, R. A., Bourke, T. L., Allen, L. E., et al. 2008, *ApJL*, 673, L151
- Kounkel, M., Hartmann, L., Loinard, L., et al. 2017, *ApJ*, 834, 142
- Kounkel, M., Covey, K., Suárez, G., et al. 2018, *AJ*, 156, 84
- Lindgren, L., Hernández, J., Bombrun, A., et al. 2018, *A&A*, 616, A2
- Loinard, L. 2013, in *IAU Symposium*, Vol. 289, *Advancing the Physics of Cosmic Distances*, ed. R. de Grijs, 36–43
- Loinard, L., Torres, R. M., Mioduszewski, A. J., et al. 2007, *ApJ*, 671, 546
- Ortiz-León, G. N., Loinard, L., Kounkel, M. A., et al. 2017a, *ApJ*, 834, 141
- Ortiz-León, G. N., Dzib, S. A., Kounkel, M. A., et al. 2017b, *ApJ*, 834, 143
- Ortiz-León, G. N., Loinard, L., Dzib, S. A., et al. 2018, *ApJ*, 865, 73
- Reid, M. J., & Honma, M. 2014, *ARA&A*, 52, 339
- Ridge, N. A., Di Francesco, J., Kirk, H., et al. 2006, *AJ*, 131, 2921
- Smith, J., Bentley, A., Castelaz, M., et al. 1985, *ApJ*, 291, 571
- Straizys, V., Černis, K., & Bartašiute, S. 2003, *A&A*, 405, 585
- Taylor, M. B. 2005, in *Astronomical Society of the Pacific Conference Series*, Vol. 347, *Astronomical Data Analysis Software and Systems XIV*, ed. P. Shopbell, M. Britton, & R. Ebert, 29
- White, G. J., Casali, M. M., & Eiroa, C. 1995, *A&A*, 298, 594
- Wilking, B. A., Gagné, M., & Allen, L. E. 2008, *Star Formation in the ρ Ophiuchi Molecular Cloud*, ed. B. Reipurth, 351